



City Research Online

## City, University of London Institutional Repository

---

**Citation:** Mahesh, V., George, J. P., Mahesh, V., Chakraborty, H., Mukunda, S. & Ponnusami, S. A. (2023). Dry-sliding wear properties of 3D printed PETG/SCF/OMMT nanocomposites: Experimentation and model predictions using artificial neural network. *Journal of Reinforced Plastics and Composites*, doi: 10.1177/07316844231188853

This is the published version of the paper.

This version of the publication may differ from the final published version.

---

**Permanent repository link:** <https://openaccess.city.ac.uk/id/eprint/31033/>

**Link to published version:** <https://doi.org/10.1177/07316844231188853>

**Copyright:** City Research Online aims to make research outputs of City, University of London available to a wider audience. Copyright and Moral Rights remain with the author(s) and/or copyright holders. URLs from City Research Online may be freely distributed and linked to.

**Reuse:** Copies of full items can be used for personal research or study, educational, or not-for-profit purposes without prior permission or charge. Provided that the authors, title and full bibliographic details are credited, a hyperlink and/or URL is given for the original metadata page and the content is not changed in any way.

---



City Research Online:

<http://openaccess.city.ac.uk/>

[publications@city.ac.uk](mailto:publications@city.ac.uk)

---

# Dry-sliding wear properties of 3D printed PETG/SCF/OMMT nanocomposites: Experimentation and model predictions using artificial neural network

Vinyas Mahesh<sup>1,2</sup> , Jerin P George<sup>1</sup>, Vishwas Mahesh<sup>3,4</sup> , Himadree Chakraborty<sup>1</sup>, Sriram Mukunda<sup>5</sup> and Sathiskumar Anusuya Ponnusami<sup>2</sup>

Journal of Reinforced Plastics and Composites

2023, Vol. 0(0) 1–12

© The Author(s) 2023



Article reuse guidelines:

[sagepub.com/journals-permissions](https://sagepub.com/journals-permissions)

DOI: 10.1177/07316844231188853

[journals.sagepub.com/home/jrp](https://journals.sagepub.com/home/jrp)



## Abstract

In this article, an attempt has been made to experimentally investigate the synergistic effect of organically modified montmorillonite (OMMT) nanoclay and short carbon fibers (SCFs) on the tribological behaviour of additively manufactured Polyethylene Terephthalate Glycol (PETG) based nanocomposites. The tribo-specimens are 3D printed using fused deposition modelling (FDM). The tribological properties, that is, specific wear rate (SWR) and coefficient of friction (CoF) of various PETG/SCF/OMMT nanocomposites were assessed by performing dry-sliding wear test. In addition, an artificial neural network (ANN) methodology is proposed to accurately predict the wear performance of PETG nanocomposites. The ANN model is trained using the datasets obtained from the experimentation. For the training of the ANN model, the Levenberg–Marquardt optimisation algorithm with 10 neurons along with a tangent sigmoid activation function is utilised. Additional experimentation was performed for arbitrary load and sliding velocity which were not used for training the ANN model and the results were compared to assess the predictive capability of the ANN model on unseen data. The proposed ANN methodology predicted the SWR and CoF with agreeable accuracy. It is believed that by adopting the proposed ANN methodology, the experimentation costs and time can be significantly reduced without compromising on the accuracy of the results.

## Keywords

Artificial neural network (ANN), additive manufacturing, PETG, wear, carbon fiber, nanoclay

## Highlights

- Tribological performance of PETG/SCF/OMMT nanocomposites are studied.
- The specimens are fabricated using additive manufacturing.
- ANN based prediction methodology is proposed.
- ANN predicted results match well with experimental results.
- Significant influence of OMMT nanoclay on wear properties is seen.

## Introduction

The use of polymer composites has increased significantly over the last decades in aerospace, automotive and wind energy industries. The extreme tailorability, specific strength and stiffness exhibited by polymer composites makes them suitable for a wide range of structural

applications. Structural components made of polymer composites in a variety of applications are exposed to extreme working conditions where wear and tear is inevitable.<sup>1</sup> Henceforth, understanding and thus improving

<sup>1</sup>Department of Mechanical Engineering, National Institute of Technology Silchar, Silchar, India

<sup>2</sup>Department of Engineering, City University of London, London, UK

<sup>3</sup>Department of Industrial Engineering and Management, Siddaganga Institute of Technology, Tumkur, India

<sup>4</sup>Department of Aerospace Engineering, Indian Institute of Science, Bangalore, India

<sup>5</sup>Department of Mechanical Engineering, Nitte Meenakshi Institute of Technology, Bangalore, India

## Corresponding author:

Vinyas Mahesh, Department of Engineering, City University of London, London EC1V 0HB, UK.

Email: [vinyas.mahesh@gmail.com](mailto:vinyas.mahesh@gmail.com)

Data Availability Statement included at the end of the article

the tribological behavior of polymer composites is crucial for successful adoption in wear-prone applications. Man *et al.*<sup>2</sup> investigated the effect of reinforcing continuous carbon fiber on the frictional characteristics of additive manufactured polyamide composites. In addition, the influence of layer deposition and fibre orientation directions on the wear behaviour was also studied. Mohammad *et al.*<sup>3</sup> investigated the influence of 3D printing process parameters on the wear performance of Polycarbonate-Acrylonitrile Butadiene Styrene composite. Sahin<sup>4</sup> studied the influence of glass and carbon fiber reinforcements on the wear behaviour of Polytetrafluoroethylenes material.

Among the many forms of thermoplastics, PETG is found to be extremely beneficial for the usage in additive manufacturing, owing to its better thermoforming and layer adhesion. PETG with short fibers are easy to fabricate and can be a natural choice for applications that do not demand extremely high mechanical properties.<sup>5</sup> Garcia *et al.*<sup>6</sup> investigated the effect of carbon fibers on the geometry of 3D printing PETG composites. Further, they optimized the geometry of the specimens using ANN. Kumar *et al.*<sup>7</sup> and Srinivasan *et al.*<sup>8,9</sup> analyzed the influence of 3D printing process parameters on the mechanical performance of PETG composites with carbon fibres. Mahesh *et al.*<sup>10,11</sup> experimentally examined the mechanical and thermal performance of nanoclay reinforced PETG/Carbon fiber composites fabricated through additive manufacturing routine. In addition, the stiffness characteristics of the same PETG composite variant is experimentally studied by Mahesh<sup>12</sup> by performing free vibration studies. Mahesh *et al.*<sup>13</sup> developed auxetic structures out of PETG/nanoclay/Carbon fiber composites and evaluated the compressive strength under quasi-static loading. Meanwhile, using ANN, the absorption characteristics of PETG composites was predicted by Vinyas.<sup>14</sup> Panneerselvam *et al.*<sup>15</sup> investigated the mechanical characteristics of 3D-printed PETG for a range of printing process parameters. Similar studies were performed by Durgashyam *et al.*<sup>16</sup> by conducting mechanical and flexural tests. Feed rate, infill density and layer thickness were taken as the process parameters in the study. Ranganathan *et al.*<sup>17</sup> studied the influence of infill density and annealing on the tribological behaviour of PETG-based composites. The study particularly states that the annealed PETG with carbon fibre with 100% infill density shows a considerable increase in wear resistance.

Even though many works have been reported on investigating the tribological properties of different polymer composites, it should be noted that the fabrication and experimentation costs and time involved are high. Therefore, it demands an alternate approach to study the wear properties without compromising on the accuracy of investigation. ANN is one such approach that predicts the

wear characteristics of the material with the help of a trained algorithm. Many researchers have adopted ANN in their studies and the outcomes of their work have been encapsulated here. Jiang *et al.*<sup>18</sup> and Zhang *et al.*<sup>19</sup> studied the wear properties of short fiber reinforced polyamide composites using ANN. Based on improved bat algorithm, Gangwar and Pathak<sup>20</sup> investigated the tribological behavior of marble dust reinforced alloy composites. Hasan *et al.*<sup>21</sup> proposed different machine learning models to understand the wear properties of aluminium composites reinforced with graphite, considering both dry and wet conditions. Varol *et al.*<sup>22</sup> used ANN approach to investigate the wear performance of Al2024–B4C composites. Using generalized regression neural networks (GRNN), Saravanakumar *et al.*<sup>23</sup> predicted the wear of AA2219-Gr matrix composites. Joshi *et al.*<sup>24</sup> optimized the wear behaviour of Aluminium hybrid composites using Antlion algorithm. Kurt *et al.*<sup>25</sup> adopted ANN to understand the wear of polyethylene composites. Sathiskumar and Rajmohan<sup>26</sup> made use of ANN methodology to optimize the wear behaviour of epoxy-based composites. Shebani and Iwnicki<sup>27</sup> applied ANN to railway wheels and predicted its wear when operated in different conditions. Suryawanshi and Behera<sup>28</sup> applied ANN methodology to dental implant and investigated their wear performance. Agbeleye *et al.*<sup>29</sup> investigated the effect of heat treatment and clay reinforcements on the wear behaviour of Aluminium composites. Pati and Satapathy<sup>30</sup> employed ANN and probed on the wear performance of slag-filled epoxy composites with glass fibers.

From the literature review, it is evident that the literature on the tribological behaviour of additive manufactured PETG composites is scarce. In specific, to our best knowledge, there are no works published on investigating the synergistic influence of reinforcing short carbon fibers (SCFs) and OMMT nanoclay on the wear behaviour of additive manufactured PETG composites. In this direction, this work makes the first attempt. More importantly, an ANN based methodology which has the potential to eliminate/reduce the fabrication and experimentation time and costs without compromising on the accuracy is proposed along with the experimental methodology. Further, the wear mechanism is studied in detail using scanning electron microscope (SEM) images.

## Materials and methods

### Materials

In this study, two main variants of PETG composites are studied, namely, (PETG + SCF) and (PETG + SCF + OMMT) composites. The raw ingredients such as PETG matrix, SCF and OMMT nanoclay reinforcements are

**Table 1.** Properties of materials.

Materials	Quality Grade	Tensile strength (maximum)	Bulk density (g/cm <sup>3</sup> )	Miscellaneous properties
PETG	SKYGREEN KN100	50 MPa	1.27	Flexural strength: 69 MPa Flexural Modulus: 2100 MPa
Carbon fibres	Code 405–100 96% natural bentonite treated	4.9 GPa	0.48	Length of Fibre: 12 mm Fiber diameter: 7 µm
Nanoclay	Cloisite SE3000	Colour White	0.45	Particle size 10 µm

procured from S K Chemical, South Korea, Arrow Technical Textiles Pvt. Ltd, India and BYK Additives and Instruments (Cloisite SE3000), India, respectively. Further details on these materials are tabulated in Table 1. In the (PETG + SCF) variant, two sub-variants with 5% SCF and 10% SCF reinforcements are fabricated. Initially, the tribological properties of these two compositions are studied and OMMT nanoclay is then reinforced to the most wear-prone (PETG + SCF) composition to get (PETG + SCF + 1% OMMT) and (PETG + SCF + 3% OMMT) variants. The addition of OMMT nanoclay is restricted to 3% to avoid any agglomeration issues. The composition of different variants of PETG composites considered in this study is shown in Table 2.

### Processing of materials

Compounding, extruding and filament winding are among the phases involved in the processing of the materials. The requisite composition of the raw materials PETG, SCF and OMMT were mechanically achieved before being mechanically combined and delivered into the screw chamber via the hopper system. The PETG/SCF/OMMT composite pellets are compounded using a twin-screw extruder of the ZV20 model, supplied by Specific Engineering and Automats, India. The extruder's screw diameter, screw length to outer diameter ratio, and screw speed were 21.5 mm, 40:1 and 600 r/min, respectively. During the compounding process, the extruder's melt temperature and pressure were 400°C and 200 bar, respectively. Further, by keeping the shaft's maximum torque value constantly at 75N-m, the continuous filaments were extracted. The temperatures of the four heating zones (feed-compression-mixing-die) while performing the compounding and extruding processes were 270-275-285°C–280°C and 175-185-205°C–200°C, respectively. Meanwhile, the compounded PETG/SCF/OMMT strands are transformed into pallets followed by pre-drying before transforming them into filament in a single screw extruder. The specifications of the

**Table 2.** Composites used in the present study.

Composite Configuration	Constituents
PC5	PETG + 5% SCF
PC10	PETG + 10% SCF
PO1C5	PETG + 1% OMMT + 5% SCF
PO3C5	PETG + 3% OMMT + 5% SCF

extruder such as screw diameter, screw length to outer diameter ratio and screw speed were 40 mm, 30:1, 90 r/min screw speed, respectively. Also, 6 kW and 1440 r/min were the motor's specified power and speed values respectively. The average diameter of the filament was 1.75 mm. Further, a laser-based optical scanner was used to verify diametrical accuracy.

### Specimen preparation

The PETG/SCF/OMMT tribo-specimens are 3D printed according to ASTM G99-05 standards, using FDM routine (Figure 1(a)). PETG/SCF/OMMT tribo-specimens are of 10mm diameter and a length of 25 mm, as seen in Figure 1(b). The infill direction of the specimen is along the sliding direction as depicted in Figure 1(c). To this end, a 3D printer developed by The Creality3D Ender-3 v2 is used with the printing specification highlighted in Table 3.

### Dry-sliding wear test

Figure (2) illustrates the setup used for wear analysis of PETG/SCF/OMMT composites. A pin-on-disc tribometer manufactured by DUCOM instruments was used for the dry sliding test, as seen in Figure 1(b).

This assembly is spun at a predetermined speed to maintain contact with a 62 HRC steel disc made of E31 hardened steel. The wear track diameter is kept constant at 35 mm for all samples. Before and after each test, the disk's surface was cleaned using acetone-soaked soft paper and

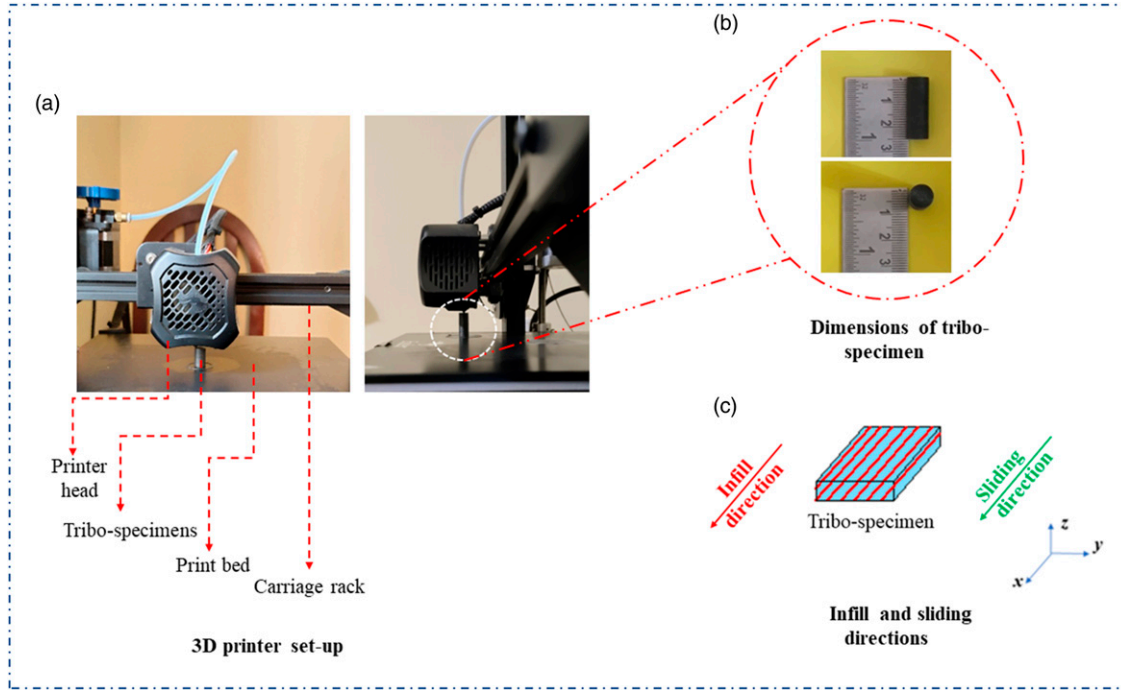


**Figure 1.** The schematics of (a) 3D printer (b) specimen dimension (c) infill direction.

**Table 3.** FDM process specifications and Values.

Specifications	Value
Nozzle temperature	220°C
Bed temperature	65°C
Print speed	45 mm/sec
Infill ratio	100%
Infill pattern	Linear
Layer height	0.16 mm
Print direction	0-degree straight lines with flat face down
Material flow rate	98%

properly dried. Alongside, 600-grit SiC paper was used to polish the pin and disc, to maintain constant surface roughness. Also, the evenness of the disc was ensured using a dial indicator. The sliding wear loss is calculated by subtracting the initial and end weights of the samples. Additionally, the wear rate and coefficient of friction were also reported. The sliding distance is determined as follows:

Sliding distance ( $L$ ) = Sliding velocity ( $v$ ) x time  
But,

$$\text{Sliding Velocity } (v) = \frac{\pi DN}{60} \quad (1)$$

therefore, equation (1) can be re-written as follows:

$$\text{Sliding distance } (L) = \frac{\pi DN}{60} \times \text{time} \quad (2)$$

where,  $D$  represents wear track diameter and  $N$  represents speed.

Meanwhile, the specific wear rate is also calculated as follows:

$$\text{Specific Wear Rate (SWR) (in } \text{mm}^3/\text{N} - \text{m)} = \frac{V}{PL} \quad (3)$$

here, ' $V$ ' is the volume of removed material ( $\text{mm}^3$ ), ' $P$ ' is the applied normal load ( $N$ ) and ' $L$ ' is the sliding distance ( $m$ )

### Artificial neural network

The ANN model has been created in MATLAB software in the present research. To train the ANN model, 540 experimental data points related to four inputs (PETG composite composition, sliding distance, load, and speed of rotation) were collected from the experimentation. Table 4 depicts the ranges of the input variables selected. The ANN model was instructed to use 70%, 15%, and 15% of the input data for training, validation, and testing, respectively. The most optimum ANN algorithm and the number of neurons were decided based on the trial-and-error method. The regression plots corresponding to different neuron numbers and algorithm types are shown in



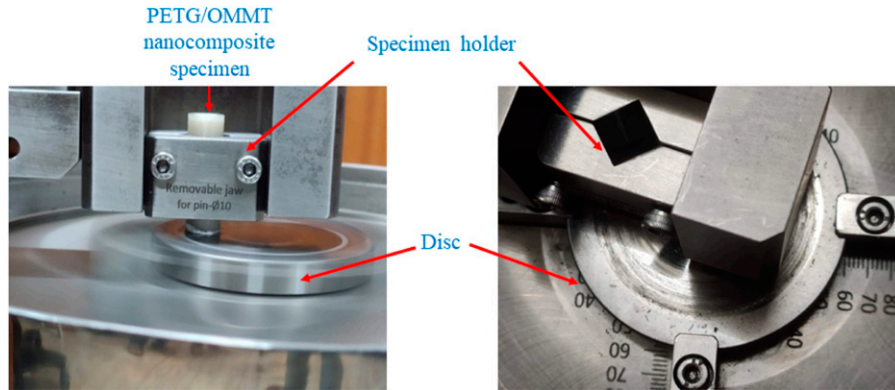


**Figure 2.** The schematics of pin-on-disc setup.

**Table 4.** The range of input parameters selected for experimentation and ANN training.

Input parameter	Range
PETG composition	PC5, PC10, PO1C5, PO3C5
Sliding distance (m)	1–1500 (in intervals of 100)
Sliding speed (rpm)	300, 600, 900
Load (N)	25, 50, 75

**Figure 3.** From this figure and **Table 5**, it is evident that the optimum value of mean square error (MSE) and correction coefficient (R) is obtained for 10 neurons. **Figure 4(a)** depicts the regression result obtained from the trained ANN optimum model with 10 neurons. Further, the capability of the trained ANN model to accurately predict the wear behaviour of PETG composites is verified. To this end, the experimentation is performed for those values of input parameters which were not used to train the ANN model. In other words, the values of input parameters such as sliding distance (1650 m), speed (950 r/min) and load (80 N) were selected outside the range used for training the ANN model. As shown in **Figure 4(b)**, the values of SWR predicted by ANN agree with that of the experimental data. **Figure 5(a)** and **(b)** depict the error histogram and the performance of the ANN model developed. The schematic representation of the ANN model with input, hidden and output layers is shown in **Figure 5(c)**.

## Results and discussion

This section discusses the tribological characteristics of additive-manufactured PETG/SCF/OMMT nanocomposite samples, considering the effect of load, sliding velocity and sliding distance. Also, the credibility of the ANN model developed to accurately predict the specific wear rate (SWR) and the coefficient of friction (CoF) is verified and compared with the experimental results.

### Effect of parameters: load and sliding velocity

Initially, the influence of load and sliding velocity on the wear behaviour of PETG composites is experimentally investigated and compared with that of the ANN predicted values. Considering the sliding distance of 500 m and sliding speed of 600 r/min, the effect of load on the SWR and CoF is studied in **Figure 6(a)** and **(b)**, respectively. It can be inferred from these figures that higher load conditions enhance the SWR and CoF. This is obvious due to the thermal softening behaviour of PETG and breakage of tribo-layers at higher loads. Further, it can also be seen from these figures that the agreement between the experimental and ANN predicted results are convincing. Similarly, the effect of sliding velocity is evaluated in **Figure 7(a)** and **(b)**. At higher speed, the SWR drastically magnifies due to the thermal softening because of frictional heating. Contradictorily, the CoF reduces owing to reduced shear strength. These effects are well captured and well predicted by the ANN model as well.

### Effect of OMMT nanoclay fillers on PETG/SCF composites

In this section, the influence of adding OMMT nanoclay on the wear behaviour of PETG/SCF composites is presented. Two variants of PETG/SCF composites, namely, PC5 (PETG +5% SCF) and PC10 ((PETG +10% SCF)) are initially assessed to select the most wear-prone composition. The different combinations of load, sliding velocity and sliding distances were selected for this experimental investigation. From **Figure 8**, it can be clearly seen that PETG +5% SCF exhibit a severe specific wear rate as opposed to PETG +10% SCF composite. This might be due to the enhanced fiber-matrix adhesion between the SCFs and PETG components exhibited by PC10 composition. Due to the obvious reasons, the CoF also follows a similar trend as noticed from **Figure 9(a)–(f)**. In addition, this variation can be attributed to the enhanced self-lubrication effect of higher percentage of SCFs. In addition, the transfer films formed at the contact also reduce the CoF. However,

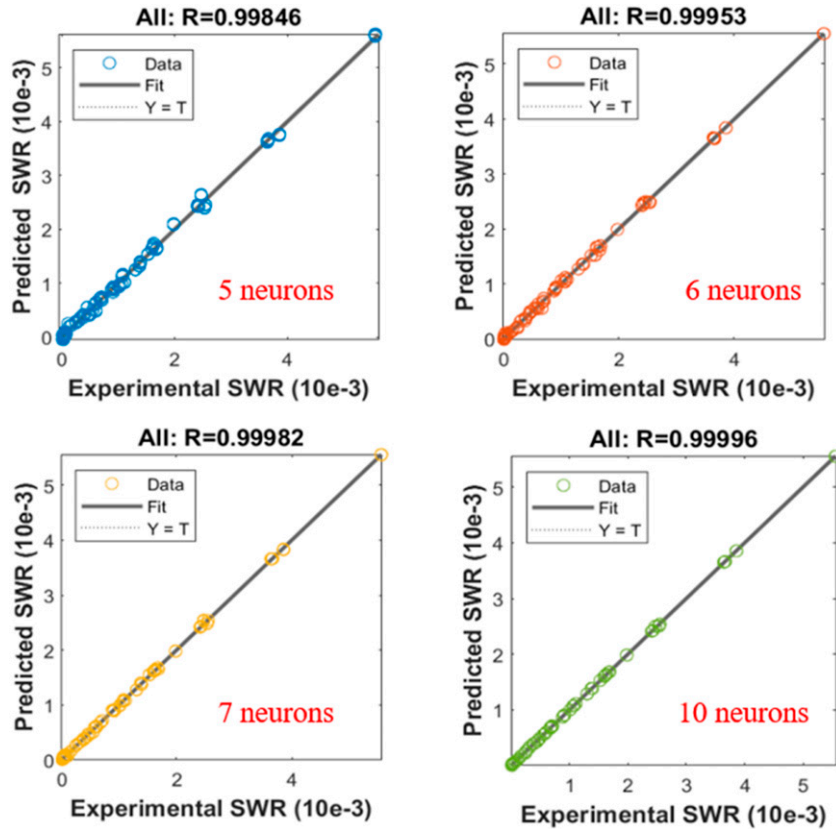


**Figure 3.** Comparison of the neuron number on the overall value of 'R' of the ANN model.

**Table 5.** The performance parameters of the ANN model.

Training parameter	Values			
No of neurons	5	6	7	10
Training time (s)	<1	<1	2	2
MSE ( $10^{-3}$ )	3.98	1.93	0.53	0.095
R	0.998	0.9994	0.9996	0.9999
Epoch	38	47	59	81

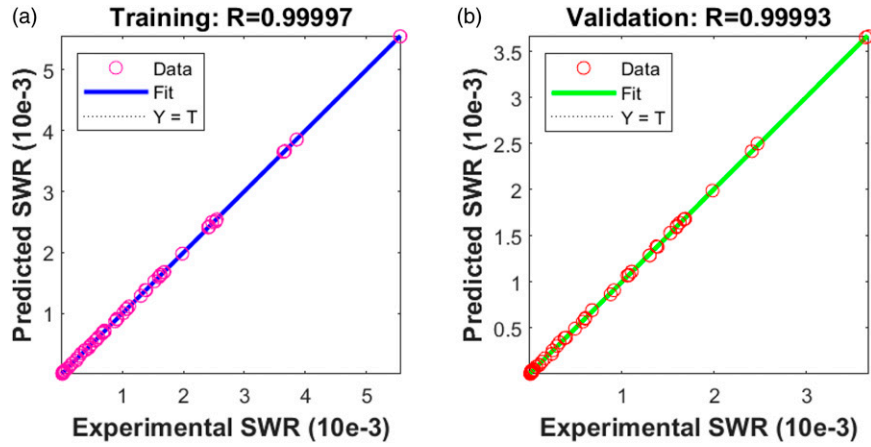
this reduction in the CoF is minimal at the higher load conditions since there is a significant amount of damage happening to the films. From this investigation it is realized that PC5 composition is more vulnerable for wear. Hence, attempts are made to enhance the tribological properties of PC5 composite through the addition of OMMT nanoclay.

From the Figure 10(a)–(f) it is clearly evident that adding/reinforcing PETG/SCF composite with nanoclay drastically reduces the specific wear rate. In other words, the tribological properties of PETG/SCF composites are significantly enhanced by adding OMMT nano fillers. This may be because the nano fillers added in the matrix cause interfacial strengthening which may lead to increased wear resistance. The high specific surface area of the nano particles leads to high interfacial adhesion between the

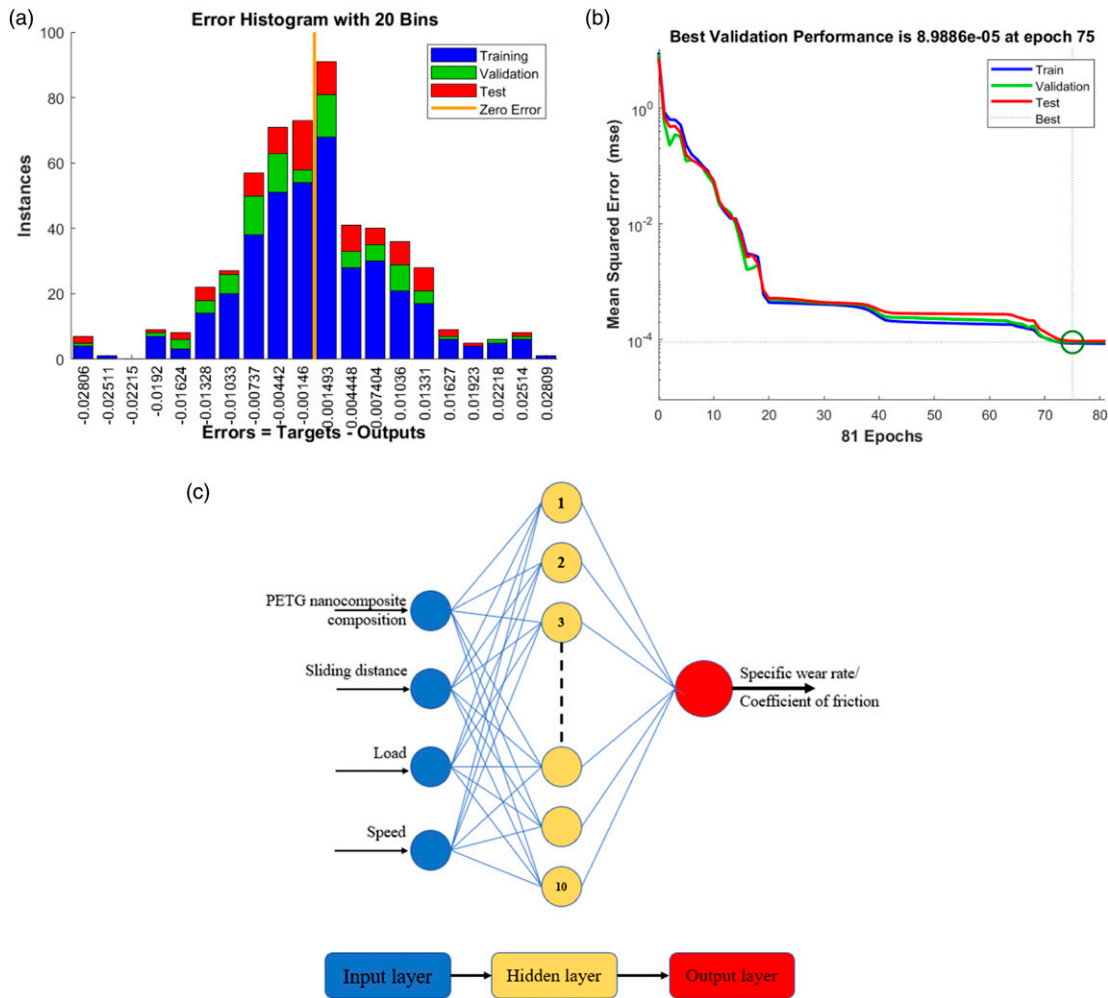
nanoparticles and the matrix. The well dispersed nano particles can act as a barrier to the soft matrix reducing the fragmentation of the polymer matrix. Also, the OMMT addition might have caused an improvement in the adhesion of transfer films to the disk thereby reducing the specific wear rates. Meanwhile, it is also evident that though the SWR for both PO1C5 and PO3C5 is lesser than PC5, the SWR is slightly higher for PO3C5 as opposed to PO1C5 variant. This can be due to the agglomeration of nano particles leading to a reduction in the surface effects of the overall composites.

Figure 11(a)–(f) show the variation of CoF, for PC5, PO1C5 and PO3C5 compositions subjected to various loads, sliding distance and velocity. It can be witnessed that the CoF is significantly reduced with OMMT nanoclay addition, as opposed to PC5. However, unlike SWR, the predominant effect of PO3C5 is seen on reducing the CoF. The decrease of CoF with increasing nanoclay addition is generally attributed to the rolling effect of nanoclay at the sliding contact. Further, the well dispersed nanoclay particles gets pulled out during the sliding and they can remain on the specimen surface. These pulled out particles can act as a roller preventing the contact between the pin and the disk reducing the CoF. It is also notable that the CoF values show less





**Figure 4.** The regression plots for (a) training and (b) validation of the optimum ANN model with 10 neurons and Levenberg–Marquardt algorithm.



**Figure 5.** The plot of (a) error histogram (b) training performance (c) architecture of the ANN model developed to predict tribological behaviour of PETG/SCF/OMMT nanocomposites.

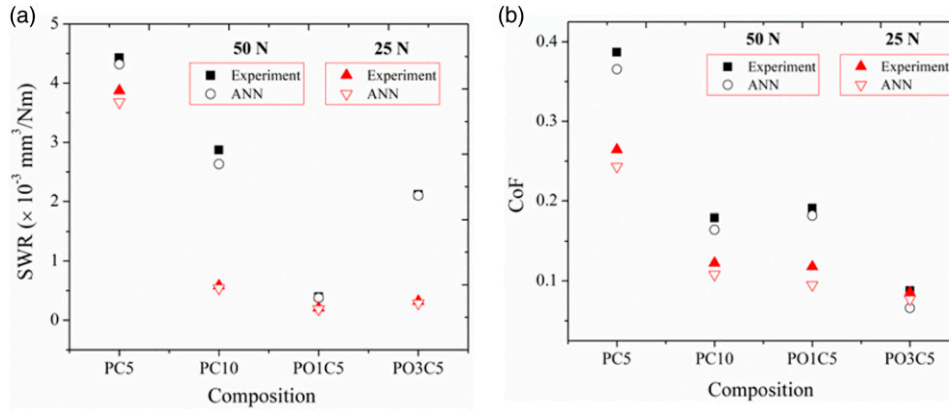


**Figure 6.** Effect of load on the (a) SWR (b) CoF of different PETG/SCF/OMMT nanocomposite samples (300 r/min, 500 m).

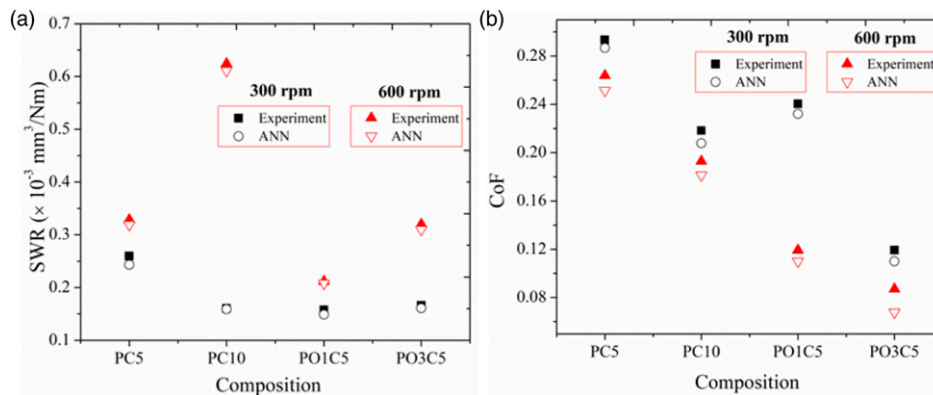


**Figure 7.** Effect of sliding velocity on the (a) SWR (b) CoF of different PETG/SCF/OMMT nanocomposite samples (25 N, 500 m).

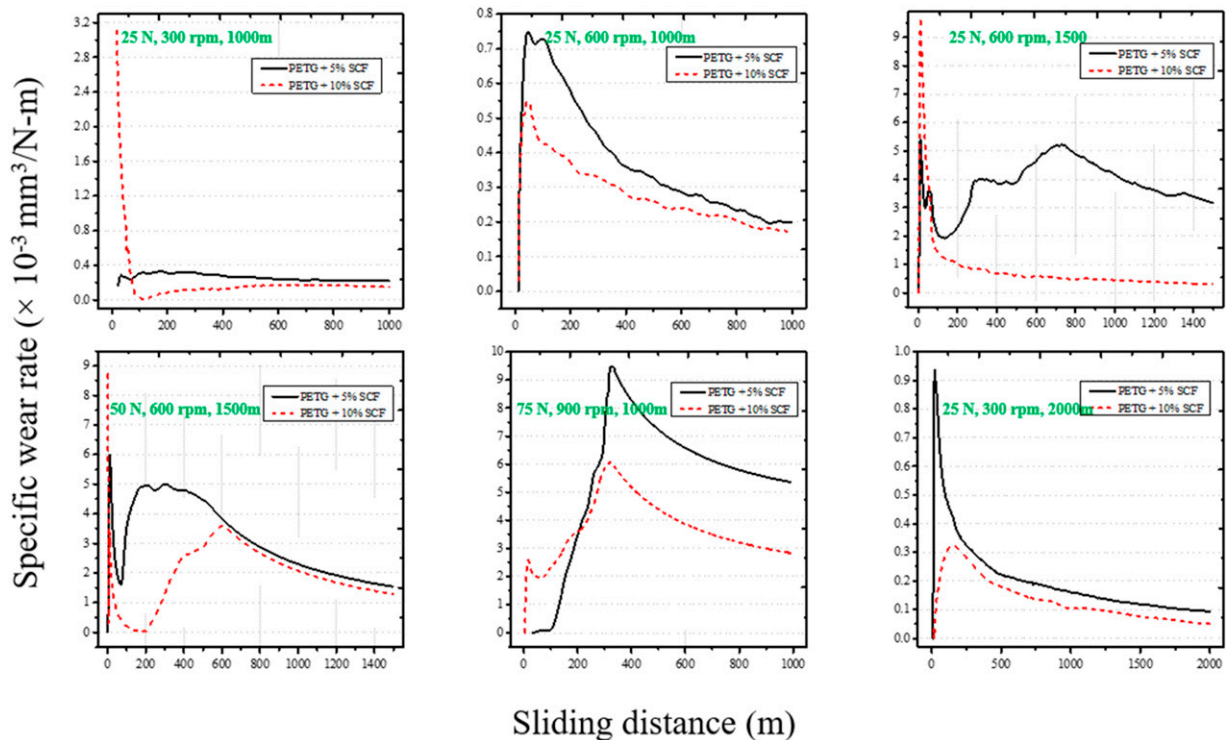


**Figure 8.** Variation of SWR of different PETG/SCF nanocomposite samples subjected to various combinations of loads, sliding velocity and sliding distance.

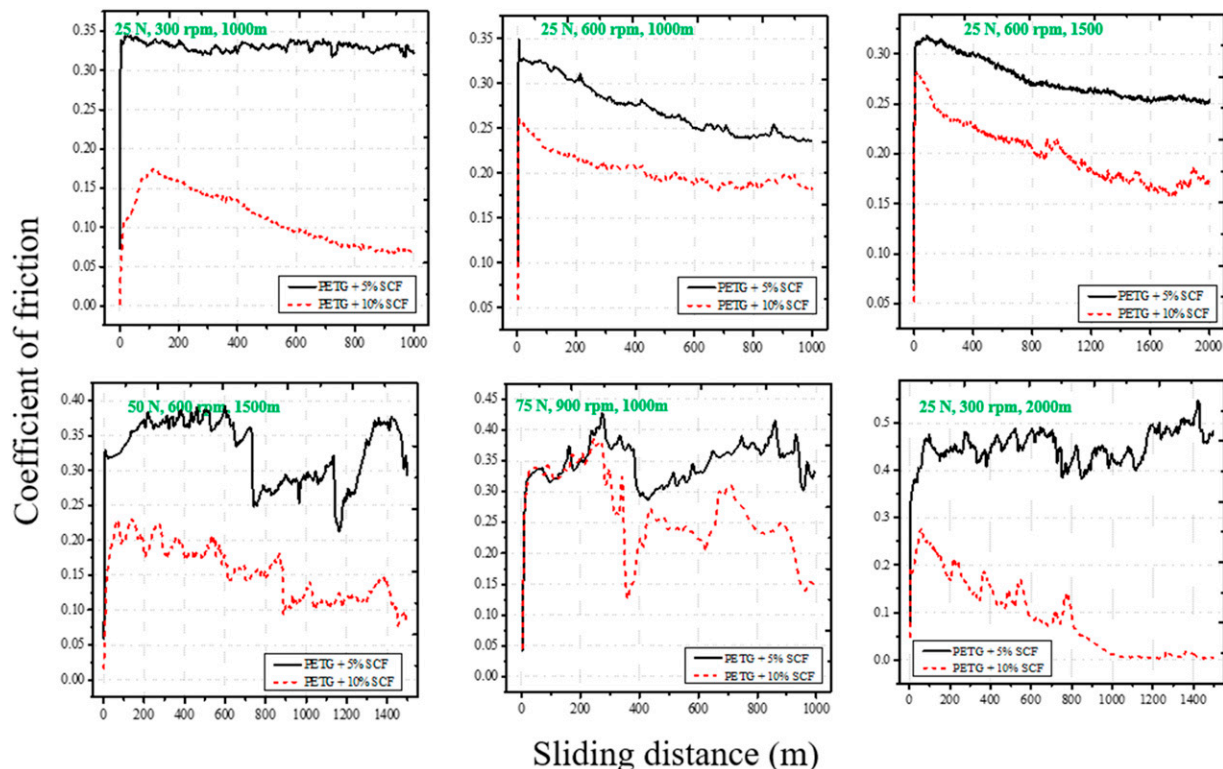


**Figure 9.** Variation of CoF of different PETG/SCF nanocomposite samples subjected to various combinations of loads, sliding velocity and sliding distance.

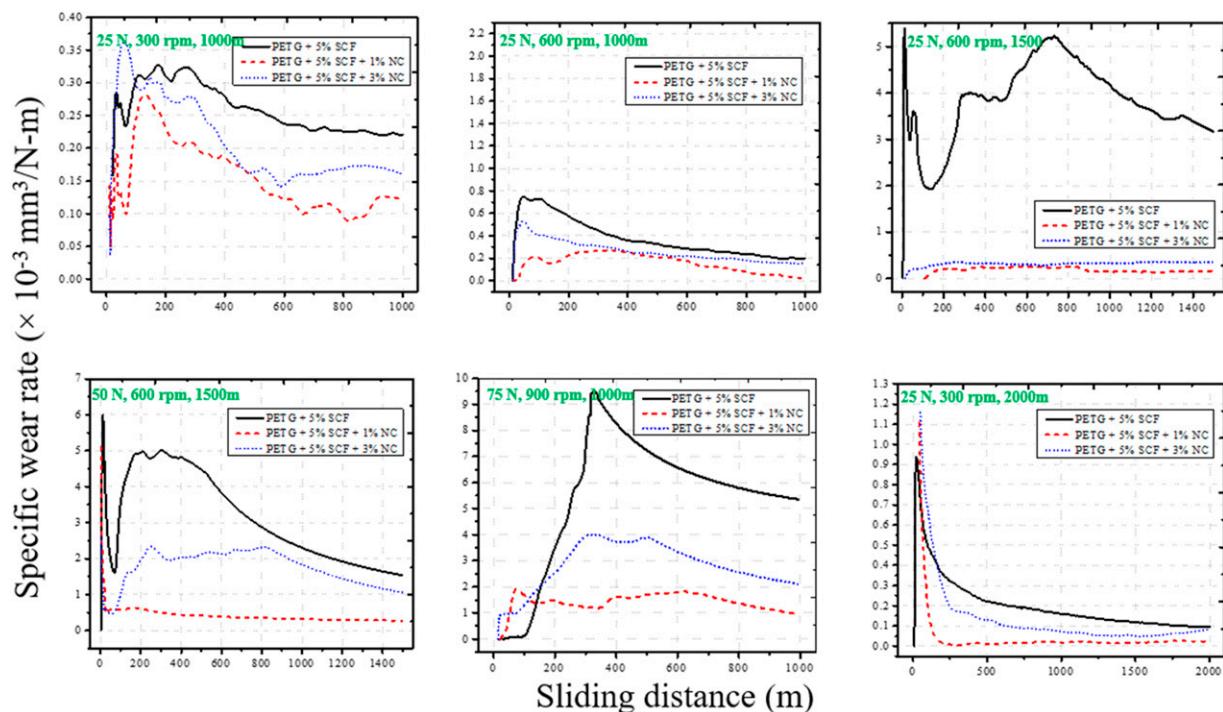


**Figure 10.** Effect of OMMT nanoclay inclusion on the SWR of different PETG/SCF nanocomposite samples subjected to various combinations of loads, sliding velocity and sliding distance.



fluctuations in Figure 11(a)–(c) where the load-rpm values are relatively lower. This can be due to the changing conditions at the interface resulting from the ploughing actions and the interface action of the debris.

Figure 12 depicts the wear mechanism involved in the proposed composites. When slid against steel counterparts, the OMMT nanoclay fillers reinforced to the neat PETG/SCF

assists the production of the transfer layer by filling the cavities present in PETG matrix. High frictional forces during sliding generate heat, potentially leading to elevated wear. Elevated temperatures can cause softening, melting, or degradation of the polymer matrix. PETG/SCF/OMMT nanocomposites with improved resistance to wear, owing to the presence of enhanced OMMT nanoparticles, exhibit reduced wear. Further,

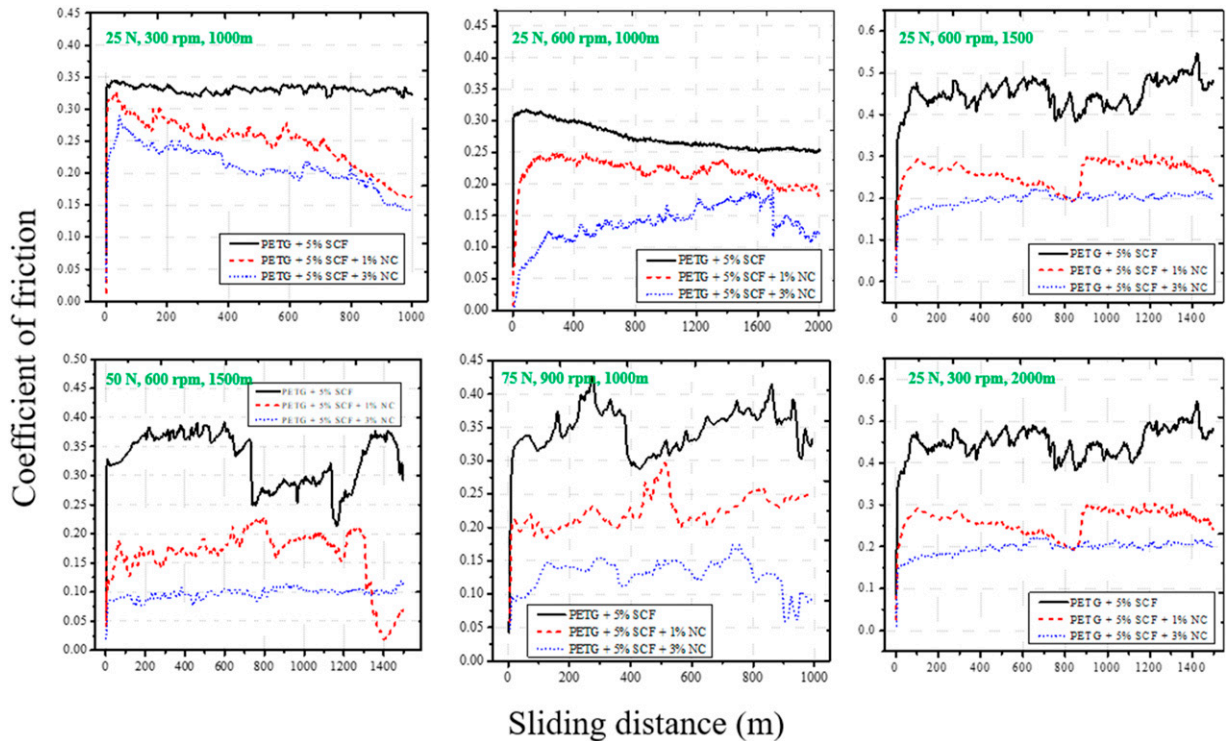


Figure 11. Effect of OMMT nanoclay inclusion on the CoF of different PETG/SCF nanocomposite samples subjected to various combinations of loads, sliding velocity and sliding distance.

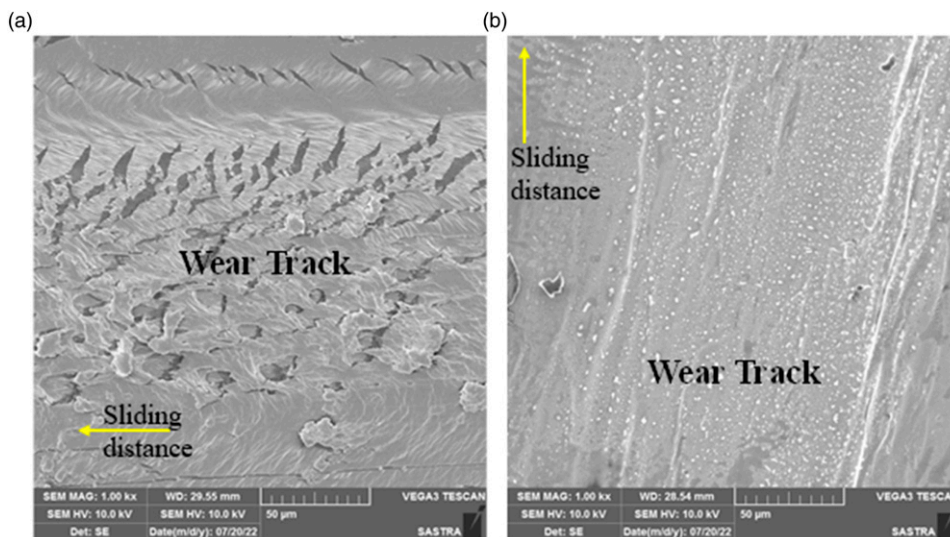


Figure 12. Wear mechanism of (a) PO1C5 (b) PO3C5 composites.

the rolling action of OMMT nanoclay particles between the specimen and the steel counterpart minimises the coefficient of friction. However, the degree of reduction depends on the percentage of nanoclay reinforcement. The OMMT nanoclay particles in PO1C5 have been dragged along the surface, plastically distorted, and crushed (Figure 12(a)). However, the surface of PO3C5 appears smoother than that of PO1C5 because it withstands higher contact pressure with a minimal wear rate. Therefore, the appearance of visible wear track is limited (Figure 12(b)).

When PO3C5 filled epoxy nanocomposites are compared to PO1C5, the wear volume loss is modest. The two surfaces of all the asperities were in touch with each other at the commencement of the slide. The asperities distorted as shear pressures were applied. The OMMT particles protrude from the sample's surface. Initially, the matrix wears down, leaving just the OMMT nanoparticles in contact with the countersurface. After extended sliding, OMMT nanoparticles adhered to the matrix, and an excess of filler concentration was observed on the composite surface. A rolling action of nanoparticles during sliding might lower shear stress, frictional coefficient and contact temperature. As a result, it was claimed that many of the hard particles were embedded in the soft polymeric transfer films on the countersurface and grooved the sample surface during the sliding process. The distance between the countersurface and the sample also increased as a result of the particle acting as spacers. As a result, the adhesion between the contacting surfaces may be reduced. As a result, the coefficient of friction of PO3C5 was always lower than the coefficient of friction of PO1C5.

Furthermore, because the nanoparticles were free to move, they were spread equally throughout the transfer films during the wear process, resulting in more uniform contact stress between the contact surfaces and, as a result, a lower stress concentration.

## Conclusions

In this article, the influence of reinforcing OMMT nanoclay fillers on the tribological behaviour of PETG/SCF composites is experimentally investigated. The tribo-specimens are fabricated through additive manufacturing. The dry-sliding wear tests were performed as per ASTM G-99 standards. From the investigation, it is revealed that compared to PC5, a better wear performance can be achieved for PC10 composition. Further, the tribological behaviour of PETG/SCF composites can be significantly enhanced by adding small weight percentage of OMMT nanoclay. The specific wear rate drastically decreased with the addition of 1% and 3% wt. OMMT nanoclay. However, the significant effect of 1% OMMT nanoclay was seen in contrast to 3% nanoclay. On the other hand, 3% inclusion of the nanoclay exhibited a predominant effect on the coefficient of friction. This is due to the enhanced rolling effect of the nanoclay between the layers. Further, using the

experimental data, an ANN methodology is proposed to accurately predict the specific wear rate and coefficient of friction of OMMT reinforced PETG/SCF composites subjected to arbitrary testing conditions. It is envisaged that such machine learning-based models combined with the experimental database may aid material scientists to reduce time and costs in materials analysis and design process.

## Acknowledgements

The financial support of the Department of Science and Technology (DST) through the Scheme for Young Scientists and Technologists (SP/YO/2021/1652) is sincerely acknowledged by the author Vinyas Mahesh.

## Declaration of conflicting interests

The author(s) declared no potential conflicts of interest with respect to the research, authorship, and/or publication of this article.

## Funding

The author(s) disclosed receipt of the following financial support for the research, authorship, and/or publication of this article: This work was supported by the Department of Science and Technology (DST) through the Scheme for Young Scientists and Technologists (SP/YO/2021/1652).

## ORCID iDs

Vinyas Mahesh  <https://orcid.org/0000-0001-8394-1321>

Vishwas Mahesh  <https://orcid.org/0000-0002-1315-9462>

## Data Availability Statement

The data given this article are the datasets generated during and/or analysed during the current study are available from the corresponding author upon reasonable request.

## References

1. Zaghoul MMY, Steel K, Veidt M, et al. Wear behaviour of polymeric materials reinforced with man-made fibres: A comprehensive review about fibre volume fraction influence on wear performance. *J Reinforc Plast Compos* 2022; 41(5-6): 215–241.
2. Man Z, Wang H, He Q, et al. Friction and wear behaviour of additively manufactured continuous carbon fibre reinforced PA6 composites. *Compos B Eng* 2021; 226: 109332.
3. Mohamed OA, Masood SH and Bhowmik JL. Analysis of wear behavior of additively manufactured PC-ABS parts. *Mater Lett* 2018; 230: 261–265.
4. Şahin Y. Analysis of abrasive wear behavior of PTFE composite using Taguchi's technique. *Cogent Engineering* 2015; 2(1): 1000510.
5. Vallejo J, García E, Núñez PJ, et al. Machinability analysis of carbon fibre reinforced PET-Glycol composites processed by additive manufacturing. *Compos Part A Appl Sci Manuf* 2023; 172: 107561
6. García E, Núñez PJ, Caminero MA, et al. Effects of carbon fibre reinforcement on the geometric properties of PETG-based filament using FFF additive manufacturing. *Compos B Eng* 2022; 235: 109766.

7. Kumar MA, Khan MS and Mishra SB. Effect of machine parameters on strength and hardness of FDM printed carbon fiber reinforced PETG thermoplastics. *Mater Today Proc* 2020; 27: 975–983.
8. Srinivasan R, Prathap P, Raj A, et al. Influence of fused deposition modeling process parameters on the mechanical properties of PETG parts. *Mater Today Proc* 2020; 27: 1877–1883.
9. Srinivasan R, Ruban W, Deepanraj A, et al. Effect on infill density on mechanical properties of PETG part fabricated by fused deposition modelling. *Mater Today Proc* 2020; 27: 1838–1842.
10. Mahesh V, Joseph AS, Mahesh V, et al. Investigation on the mechanical properties of additively manufactured PETG composites reinforced with OMMT nanoclay and carbon fibers. *Polym Compos* 2021; 42(5): 2380–2395.
11. Mahesh V, Joseph AS, Mahesh V, et al. Thermal characterization of organically modified montmorillonite and short carbon fibers reinforced glycol-modified polyethylene terephthalate nanocomposite filaments. *Polym Compos* 2021; 42(9): 4478–4496.
12. Mahesh V. Experimental investigation on the dynamic response of additive manufactured PETG composite beams reinforced with organically modified montmorillonite nanoclay and short carbon fiber. *Polym Compos* 2021; 42(10): 5021–5034.
13. Mahesh V, Maladkar PG, GanguSadaram SSet al. Experimental investigation of the in-plane quasi-static mechanical behaviour of additively manufactured polyethylene terephthalate/organically modified montmorillonite nanoclay composite auxetic structures. *J Thermoplast Compos Mater* 2022; 1–21, doi: <https://doi.org/10.1177/08927057221147826>.
14. Vinyas M. ANN based prediction of the absorption characteristics of additive manufactured glycol-modified polyethylene terephthalate nanocomposites reinforced with short-carbon fibers and nanoclay fillers. *Polymer Composite* 2023; 1–17, doi: <https://doi.org/10.1002/pc.27337>.
15. Panneerselvam T, Raghuraman S and Krishnan NV. Investigating mechanical properties of 3D-printed polyethylene terephthalate glycol material under fused deposition modeling. *J Inst Eng: Series C* 2021; 102(2): 375–387.
16. Durgashyam K, Reddy MI, Balakrishna A, et al. Experimental investigation on mechanical properties of PETG material processed by fused deposition modeling method. *Mater Today Proc* 2019; 18: 20522059.
17. Ranganathan S and Palanivelu R. Enhancing the tribological properties PETG and CFPETG composites fabricated by FDM via various infill density and annealing (No. 2020-28-0429). SAE Technical Paper. *Technical Paper: International Conference on Advances in Design, Materials, Manufacturing and Surface Engineering for Mobility*. SAE International, 2020.
18. Jiang Z, Zhang Z and Friedrich K. Prediction on wear properties of polymer composites with artificial neural networks. *Compos Sci Technol* 2007; 67(2): 168–176.
19. Zhang Z, Friedrich K and Velten K. Prediction on tribological properties of short fibre composites using artificial neural networks. *Wear* 2002; 252(7-8): 668–675.
20. Gangwar S and Pathak VK. Dry sliding wear characteristics evaluation and prediction of vacuum casted marble dust (MD) reinforced ZA-27 alloy composites using hybrid improved bat algorithm and ANN. *Mater Today Commun* 2020; 25: 101615.
21. Hasan MS, Kordijazi A, Rohatgi PK, et al. Machine learning models of the transition from solid to liquid lubricated friction and wear in aluminum-graphite composites. *Tribol Int* 2022; 165: 107326.
22. Varol T, Canakci A and Ozsahin S. Artificial neural network modeling to effect of reinforcement properties on the physical and mechanical properties of Al2024–B4C composites produced by powder metallurgy. *Compos B Eng* 2013; 54: 224–233.
23. Saravanakumar A, Rajeshkumar L, Balaji D, et al. Prediction of wear characteristics of AA2219-Gr matrix composites using GRNN and Taguchi-based approach. *Arabian J Sci Eng* 2020; 45(11): 9549–9557.
24. Joshi AG, Manjaiah M, Basavarajappa S, et al. Wear performance optimization of SiC-Gr reinforced Al hybrid metal matrix composites using integrated regression-antlion algorithm. *Silicon* 2021; 13: 3941–3951.
25. Kurt HI and Oduncuoglu M. Application of a neural network model for prediction of wear properties of ultrahigh molecular weight polyethylene composites. *International Journal of Polymer Science* 2015; 2015: 315710.
26. Satish Kumar D and Rajmohan M. Optimizing wear behavior of epoxy composites using response surface methodology and artificial neural networks. *Polym Compos* 2019; 40(7): 2812–2818.
27. Shebani A and Iwnicki S. Prediction of wheel and rail wear under different contact conditions using artificial neural networks. *Wear* 2018; 406: 173–184.
28. Suryawanshi AS and Behera N. Prediction of abrasive wears behavior of dental composites using an artificial neural network. *Comput Methods Biomech Biomed Eng* 2022; 26: 1–11.
29. Agbeleye AA, Esezobor DE, Agunsoye JO, et al. Prediction of the abrasive wear behaviour of heat-treated aluminium-clay composites using an artificial neural network. *J Taibah Univ Sci* 2018; 12(2): 235–240.
30. Pati PR and Satapathy A. Prediction and simulation of wear response of Linz–Donawitz (LD) slag filled glass–epoxy composites using neural computation. *Polym Adv Technol* 2015; 26(2): 121–127.